The Evaluation of the Boundary Vorticity by URANS and LES Methods

Ion MALAEL[1], Horia DUMITRESCU[2], Vladimir CARDOS*,[2]

*Corresponding author
[1]National Research and Development Institute for Gas Turbine, COMOTI, Bucharest, Romania
ion.malael@comoti.ro
*,[2]"Gheorghe Mihoc – Caius Iacob" Institute of Mathematical Statistics and Applied Mathematics of the Romanian Academy
Calea 13 Septembrie no. 13, 050711 Bucharest, Romania
dumitrescu.horia@yahoo.com, v_cardos@yahoo.ca*

DOI: 10.13111/2066-8201.2015.7.4.10

Received: 27 May 2015 / Accepted: 02 August 2015

Abstract: *The role of concentrated vorticity in fluid dynamics phenomena, concerning both the vorticity creation at the boundary and the response to the flow field is not wholly understood. The Lighthill describes the vorticity production at a solid boundary as a slow diffusion of the vorticity similar to the Fourier heat conduction. In the paper it is shown that this mechanism associated to URANS method is not applied to the concentrated vorticity case, and the LES method better reproduces the flows involving concentrations vorticity.*

Key Words: *Boundary layer, Velocity profile, URANS, LES*

1. INTRODUCTION

The role of vorticity, defined as the curl of the velocity vector, in understanding various fluid dynamics phenomena, is well established. Lighthill in his wide-ranging introduction to the boundary-layer theory provided an extensive description of vorticity dynamics in a variety of flows [1]. He was also the first to introduce the concept of vorticity flux density and to define the vorticity production at solid/fluid boundaries in a two-dimensional viscous flow by analogy to Fourier's heat conduction law as

$$\frac{1}{\rho}\frac{\partial p}{\partial x} = \nu \frac{\partial \omega}{\partial y} \text{ on } \partial B, \tag{1}$$

where ω is the transverse vorticity over the two-dimensional wall ∂B and ν the viscosity. Hence, the vorticity flux is directly related to the pressure gradient at wall although the transport equation of vorticity contains no pressure. Therefore, the pressure gradients associated with the velocity flow field are necessary for his model of vorticity diffusion into the flow at the solid process. In a recent paper [3], in contrast to Lighthill's diffusion mechanism, Fig. 1 [1], [2], a wave mechanism for vorticity change at the wall beneath a flow has been proposed, Fig. 2. The vorticity-boundary interaction problem has been considered as an impact process where the momentum exchange between colliding bodies within a short

term of contact, produces the concentrated vorticity at physical surfaces in the form of point vortices on the boundary. Such rapid loading in the contacting area is a vorticity source where waves are emitted propagating as the fast longitudinal *L*-wave and the slower transverse *T*-wave with an intricate pattern, as seen in Fig 2. The visco-elastic type fluid and the concept of torsion vorticity wires are used to describe the onset/relaxation of vorticity at boundaries caused by the surface-fluid impact.

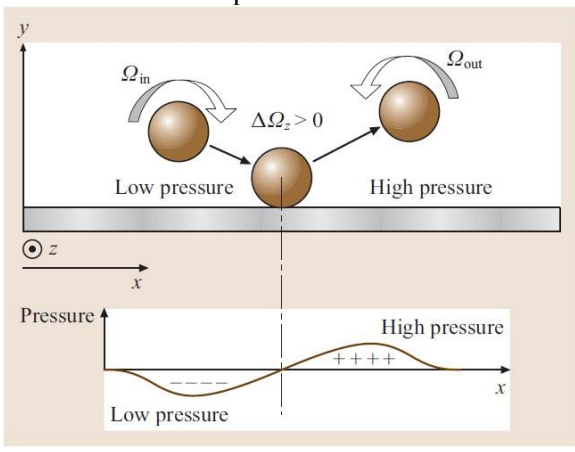

Figure 1 – Lighthill's mechanism of vorticity change at the wall beneath a flow

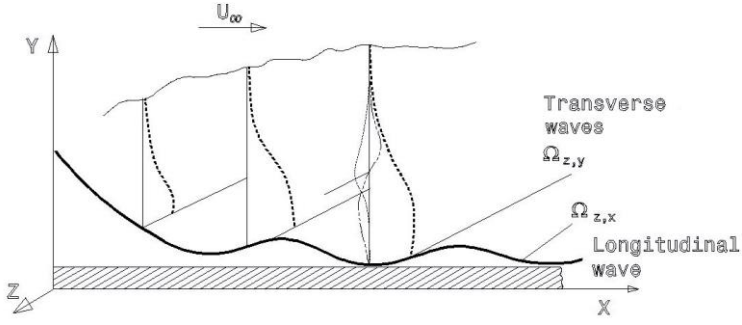

Figure 2 – The wave mechanism of vorticity transport at the wall beneath a flow

The CFD numerical techniques, i.e. URANS and LES are compared to determine their suitability in the prediction of the fluctuations of flow field induced by the concentrated vorticity in very large Reynolds number flows.

2. PHYSICS OF START-UP FLOW

Any flow that starts from rest and interacts with a physical surface experiences a kind of thixotropic effects due to the two colliding bodies within a short time of contact. Thixotropy comes about first because of the finite time taken for the shear-induced change in microstructure to take place. The microstructure is brought to a new equilibrium by competition between the processes of tearing apart by stress and flow-induced collision. Then, the Brownian motion is able to move the elements of the microstructure slowly around to more favourable positions and thus rebuilding the structure. The whole process, completely reversible [2], gives rise in fluid to internal vorticity waves: an exciting longitudinal wave (L) depending on the Reynolds number, followed by a number of dispersive transverse waves (T). At very large Reynolds numbers in the range of values

($\nu_0^{-1} - e^2\nu_0^{-1}$), the vorticity is rolled up into concentrated conglomerates occurring unsteady fluctuations of the fluid. The CFD codes are evaluated against experimental data for three known flows: a flat plate at zero incidence [4] airfoil at high AOA (angle of attack) [5]; 3-blade SBVAWT (straight-bladed-vertical-wind-turbine) [6].

3. FLOW SIMULATION

Numerical simulations are performed using FLUENT with the aim of reproducing the experimental works [4], [5], [6], focusing on the concentrated vorticity. The domain is discretized using hexahedral elements incorporating recommendations based on the wall approach, where the half of total cell (10^6) are placed within the elastic sublayer defined by

$$\eta e^{1-\eta} = \eta^{1/e}, \eta = \frac{y}{\delta}, \tag{2}$$

where δ is the boundary layer thickness.

The unsteady RANS solutions are obtained using standard *k*-ε RSM turbulence models and a non-dimensional time step of $4 \cdot 10^2$ for the unsteady solution. The equations are

$$\frac{\partial \overline{u}_e}{\partial x_i} = 0, \tag{3}$$

and

$$\frac{\partial \overline{u}_e}{\partial t} + \overline{u}_e \frac{\partial \overline{u}_e}{\partial x_j} = -\frac{1}{\rho}\frac{\partial \overline{p}}{\partial x_i} + \nu \frac{\partial^2 \overline{u}_e}{\partial x_j^2} - \overline{u_j' \frac{\partial u_e'}{\partial x_j}}. \tag{4}$$

In RANS the flow properties are disintegrated into their mean and fluctuating components and integration over time (time-averaging) is performed. In URANS, an addition unsteady term is present in the momentum equation (4).

In LES, the dynamic Smagorinsky-Lily Sub-grid Scale (SGS) model is chosen. Bounded central differencing scheme for momentum, 2nd order time advancement and 2nd order upwind for energy transport equation are chosen. A dimensionless time-step of 2.5 10^{-3} was chosen. The LES equations are (3) and

$$\frac{\partial \overline{u}_e}{\partial t} + \overline{u}_e \frac{\partial \overline{u}_e}{\partial x_j} = -\frac{1}{\rho}\frac{\partial \overline{p}}{\partial x_i} + \nu \frac{\partial^2 \overline{u}_e}{\partial x_j^2} - \frac{\partial \tau_{ij}}{\partial x_j}. \tag{5}$$

In LES, the over-bar indicates spatial filtering, and not time-averaging as is the case of URANS. It is worth identifying that the filtered momentum equation is similar to the URANS equation.

The spatial-filtering is an integration just like time-averaging, the difference being that the integration is in space and not over time as in the case of URANS. Further details of the modelling techniques can be found in the FLUENT documentation [7].

4. RESULTS AND DISCUSSION

Numerical results obtained from unsteady RANS and transient LES are presented focusing on the comparison of numerical results obtained for three test-flows involving vorticity concentrations in experimental conditions.

A. Flat plate at zero incidence

This case was the first example of the Prandtl boundary-layer equations treated by Blasius [4]. Recently, it has been found the full Blasius solution which confirms the concept of the visco-elastic fluid to describe various vorticity-boundary interactions. Thus, Fig. 3 illustrates the concentrated vorticity contours at Re = 5 10^5, which demonstrates the quantitative comparison between the two different CFD techniques. It is observed that LES not only predicts much better than URANS, but also reproduces much more consistent results: in contrast to the URANS results which show a diffusion process of vorticity, LES predicts well the behaviour by vorticity waves.

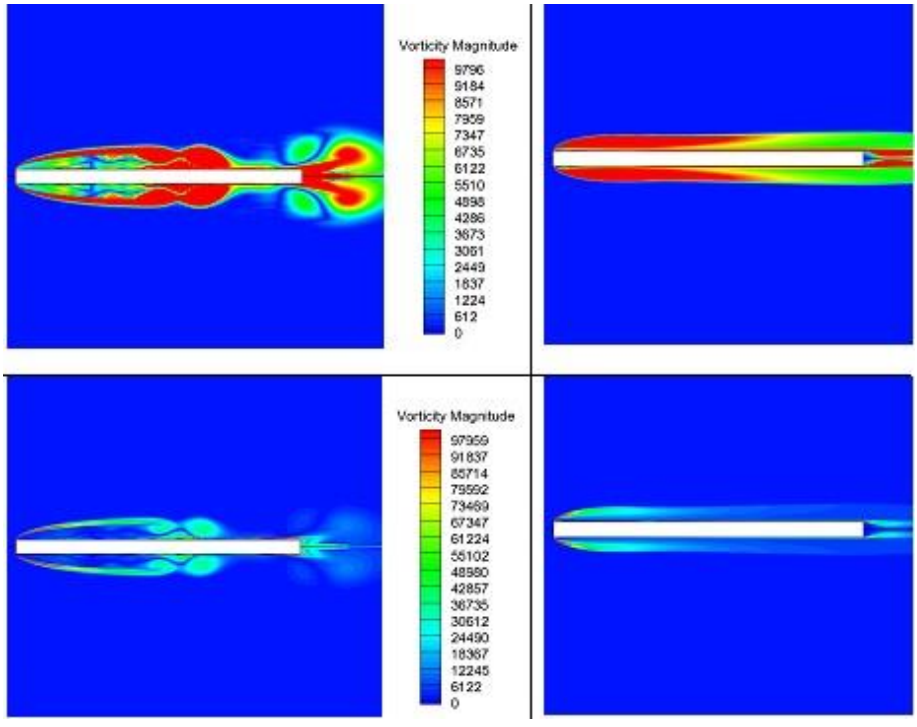

Figure 3 – Flat plate at zero incidence Re = 5 10^5.

B. Airfoil at high AOA

The CFD simulation of airfoil flow with an AOA higher than 45^0 at very large Reynolds numbers is rarely discussed in the literature. However, VAWT blades encounter a very high AOA as they rotate at a low TSR (tip speed ratio). Fig. 4 shows the transient vorticity contours at $\alpha = 20^0$, 40^0, 60^0 and 90^0 from URANS and LES.

The URANS produced large and smooth vortex shedding and prevented the vortices from diffusing into smaller ones, whereas the LES computation reproduced the breakup of these large separation bubbles.

In 2D flow, vorticity is transported only in plane, which results in concentration in massive separation vortices. On the other hand, the URANS method is intended for modelling the turbulence by Reynolds time-averaged treatment, in which the Reynolds-stress term, regarded as energy transported through turbulence fluctuation, is unresolved but modelled using time-averaged terms. Therefore, it is unsurprising that only large periodic vortices shedding are reproduced by URANS.

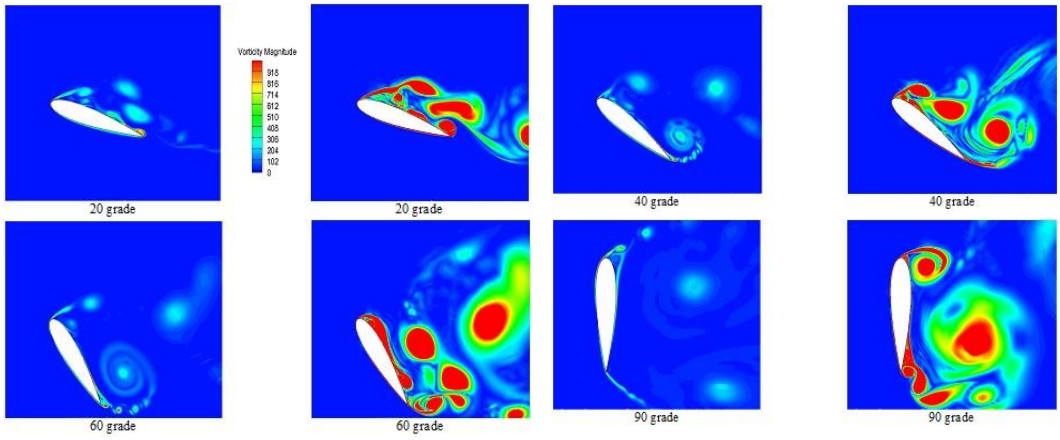

Figure 4 – Airfoil at high AOA: 20^0, 40^0, 60^0, 90^0.

C. 3-bladed SBVAWT

Figure 5 a, b shows the computed vorticity field in the vicinity of the airfoil and $\theta = 90^0$ and $\theta = 120^0$ from URANS and LES.

Compared with the experimental results (Fig. 5 a,b,c), the URANS underestimates the generation and shedding of vorticity at the leading edge (the half of the aerofoil); leading edge shed vorticity is only located at the first.

The URANS is able to better approximate the average vortical distribution, including simulating the rolling up of the wake, but the vorticity distribution is still a single continuous vortical field, instead of the distribution of several small vortices, as observed in the experiments (Fig. 5c). Unlike URANS, in LES the equations are not Reynolds averaged in time, but are space filtered (average in volume).

In this simulation, (Fig. 5b) the large shedding of leading-edge vorticity and the roll-up of the trailing-edge wake are simulated; yet, the location of the vorticity shed at the leading edge covers a larger area than what was observed in the experimental results and the roll-up of the trailing-edge wake occurs too early in the rotation.

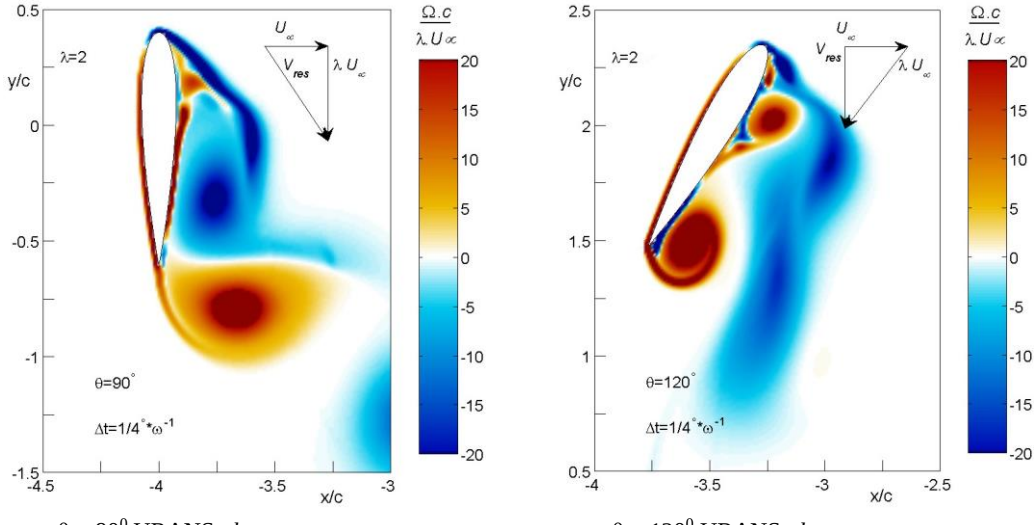

$\theta = 90^0$ URANS k -ε

$\theta = 120^0$ URANS k -ε

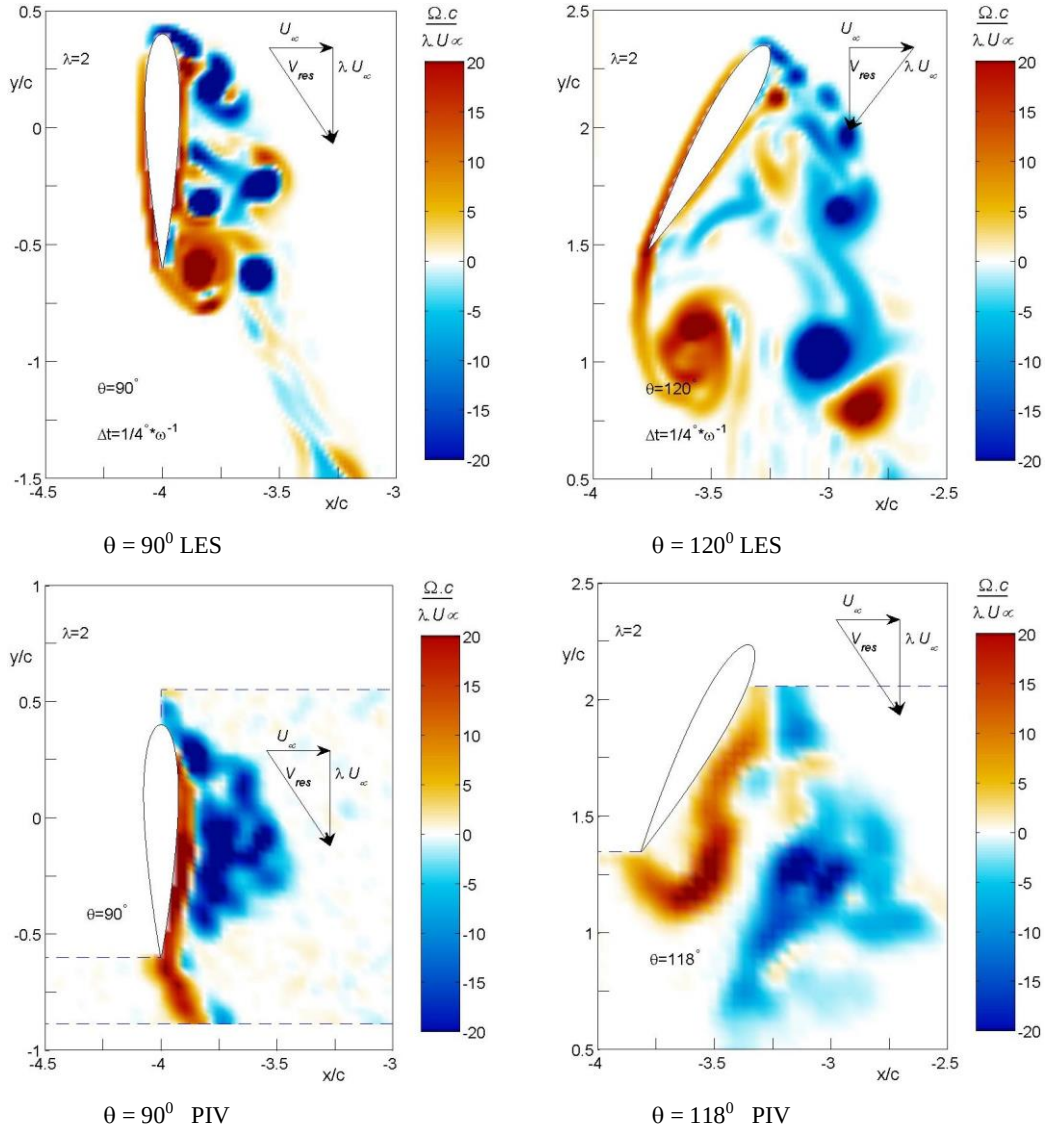

θ = 90^0 LES θ = 120^0 LES

θ = 90^0 PIV θ = 118^0 PIV

Figure 5 a, b, c – Three-bladed SBVAWT.

5. CONCLUSIONS

Two CFD techniques, namely 2D Unsteady Reynolds-Averaged Navier-Stokes (URANS) and Large Eddy Simulations (LES) were employed for the simulation of three flows, involving strong vorticity concentrations.

For all considered flows, URANS was unable to accurately account for the fluctuations of the vorticity field, although solving for the transient solution, as it is limited to the externally induced fluctuations (B, C cases).

Contrary to URANS, in LES the equations are not Reynolds averaged in time, but are directly solved for the larger scales of turbulence. LES produced the solutions most accurately and consistently, because it resolves the unsteady fluctuations that capture the vorticity mixing process from flow.

ACKNOWLEDGEMENT

This work was realized through the Partnership programme in priority domains – PN II, developed through support provided from ANCS CNDI – UEFISCDI, project no. PN-II-PT-PCCA-2011-32-1670.

This work was presented at ***3rd International Workshop on Numerical Modelling in Aerospace Sciences, NMAS 2015****, 06-07 May 2015, Bucharest, Romania,* (held at INCAS, B-dul Iuliu Maniu 220, sector 6).

REFERENCES

[1] M. J. Lighthill, *Introduction: Boundary layer theory, in Laminar Boundary Theory*, ed. by L. Rosenhead, Oxford University Press, Oxford, pp. 46-113 1963.

[2] C. Tropea, L. A. Yarin, F. J. Foss, Eds, *Handbook of Experimental Fluid Mechanics*, Springer-Verlag, 2007.

[3] H. Dumitrescu, V. Cardos, Vorticity waves in shear flows, *INCAS BULLETIN*, (online) ISSN 2247–4528, (print) ISSN 2066–8201, ISSN–L 2066–8201, Vol. **7**, Issue 1, DOI: 10.13111/2066-8201.2015.7.1.5, pp. 51-56, 2015.

[4] H. Schlichting, K. Gersten, *Boundary Layer Theory*, Springer-Verlag, 2000.

[5] N. N. Sorensen, J. A. Michelsen, Drag prediction for blades at high angle of attack using CFD, J. *Sol. Energy Eng.*, Vol. **126**, pp. 1011-1016, 2004.

[6] C. J. S. Ferreira, A. Van Zuijlen, H. Bijl, G. Van Bussel, G. Van Kuik, Simulating dynamic stall in a two-dimensional vertical-axis wind turbine: verification and validation with particle image velocimetry data, *Wind Energy*, Vol. **13**, pp. 1-17, 2010.

[7] *** ANSIS Fluent-Commercially available CFD software package based on the finite volume method, www.ansys.com, 2011.